# Electrodeposition of copper (II) sulfide and zinc sulfide onto polycrystalline gold electrode

## Bakır (II) sülfür ve çinko sülfürün polikristalin altın elektrot üzerine elektrodepozisyonu

**Özge Sürücü** [1,2] ,  **Serdar Abacı** [1,3*]

[1] Department of Chemistry, Faculty of Science, Hacettepe University, Ankara, TURKEY
[2] Department of Chemistry, Faculty of Science, Ege University, Izmir, TURKEY
[3] Advanced Technologies Application and Research Center, Hacettepe University, Ankara, TURKEY
*Sorumlu Yazar / Corresponding Author* *: sabaci@hacettepe.edu.tr

**Abstract**

An electrodeposition-based process was developed in this work. Electrochemical atomic layer epitaxy (ECALE) and co-deposition methodologies were employed to grow copper (II) sulfide (CuS) and zinc sulfide (ZnS) thin films as photovoltaic semiconductors on polycrystalline gold electrode. The deposition potentials of copper (Cu), zinc (Zn) and sulfur (S) were defined separately by cyclic voltammetry. Thin films were created from an electrolyte containing copper (II) sulfate ($CuSO_4$), sodium sulfur ($Na_2S$) and zinc sulfate ($ZnSO_4$) in ethylenediaminetetraacetic acid (EDTA) using both cyclic voltammetry and bulk electrolysis techniques. The influence of bath temperature at the deposition potential was studied to determine the crystallinity of deposits. From the chronoamperometry results including the transients obtained within the under potential region, the nucleation and growth process of deposits were estimated. In this way, an electrodeposition-based method for CuS and ZnS semiconductors in a comparable basis was improved on polycrystalline gold substrate.

*Keywords:* Copper, Zinc, Underpotential deposition, Co-deposition, ECALE.


**Öz**

Bu çalışmada, elektrodepozisyona dayanan bir sistem geliştirilmiştir. Elektrokimyasal atomik tabaka epitaksi (ECALE) ve ko-depozisyon metodolojileri, bakır (II) sülfür (CuS) ve çinko sülfür (CuS) ince filmlerinin polikristalin altın elektrot üzerinde fotovoltaik yarı-iletkenler olarak büyütülmesi için kullanılmıştır. Bakır (Cu), çinko (Zn) ve kükürdün (S) biriktirme potansiyelleri dönüşümlü voltametri ile ayrı ayrı belirlenmiştir. İnce filmler etilendiamin tetra asetik asit (EDTA) içinde bakır (II) sülfat ($CuSO_4$), sodyum sülfür ($Na_2S$) ve çinko sülfat ($ZnSO_4$) içeren bir elektrolit çözeltisinden hem dönüşümlü voltametri hem de bulk elektroliz teknikleri kullanılarak oluşturulmuştur. Biriktirme potansiyelindeki sıcaklık etkisi katmanların kristalliğinin belirlenmesi için çalışılmıştır. Potansiyel altı alan içerisinde elde edilen geçişleri kapsayan kronoamperometri sonuçlarından, katmanların çekirdekleşme ve büyüme süreçleri değerlendirilmiştir. Böylece, CuS ve ZnS yarı iletkenleri için karşılaştırma esaslı elektrodepozisyona dayanan bir metot polikristalin altın substratta geliştirilmiştir.

*Anahtar Kelimeler:* Bakır, Çinko, Potansiyel altı depozisyonu, Ko-deposizyon, ECALE.

## 1. Introduction

The underpotential deposition (UPD) of metals enables specially controlled modifications on the catalyst surface, so it has been extensively studied in electronic industry as a well-known phenomenon [1]. Such a process is applied by the interactions between ad-atoms and substrate (SS) depositing a metal (M) at a potential more positive than the Nernst potential for the couple $M/M^{n+}$ [2].

Electrochemical atomic layer epitaxy (ECALE) is one of the UPD-based electrochemical deposition methods and it works with the sequential and separate UPD of different elements [3]. As a pioneer of UPD-based electrochemical techniques, ECALE has been widely applied for the electrochemical growth of well-ordered semiconductor materials [4]. In another UPD-based electrochemical technique, UPD-based co-deposition has focused on the electrodeposition of a compound from the same solution at a common UPD potential [5]. Such a practical and applicable method can be successfully used in the production of nanostructured semiconductors [6].

The mainly used substrates are gold (Au) [7], platinum (Pt) [8], silver (Ag) [9] and copper (Cu) [10] in the form of single and polycrystalline for photovoltaic applications. Most of the applications are aimed at chalcogenide compounds such as cadmium telluride (CdTe) and copper indium selenide ($CuInSe_2$) containing tellurium (Te), indium (In) and selenium (Se) as anode material, but sulfides of Cu and zinc (Zn) has been worked out less [11]. Electrodeposition of Zn on metals are widely used on industrial scale as corrosion protective coatings, but the electrochemical process of zinc in various electrolytes is not well-known [12]. Initial studies about Zn electrodeposition have focused on overvoltage, Zn salts, bath temperature, current densities and additives [8]. A little attention has been given for the nucleation kinetics and characterization of Zn deposition on polycrystalline electrodes [13].

The UPD of sulfur (S) is one of the most intensively investigated topic of semiconductor family. A great deal of attention has focused on understanding the kinetics of S monolayer deposition [14]. Zinc sulfide (ZnS) is among the most attractive II–VI compound semiconductors for photovoltaic applications [15]. Nevertheless copper (II) sulfide (CuS) systems are particularly interesting as active material for solar energy conversion, sensors, photocatalysis and light emitting devices, but these systems exist of different stoichiometry and crystal structure in very limited solid solutions [16]. Therefore, additional insight into the voltammetric behaviors of ZnS and CuS in the UPD range is necessary to understand the semiconducting properties of coated surfaces. Most of the studies in literature focus on one technique as ECALE or co-deposition. The choice of best nucletion and growth mechanism must be offered in literature. Also, the superiority of polycrystalline surfaces will help semiconductor industry as an easy accessible materials.

In the present paper, the electrodepositions of Cu and Zn in conjunction with S onto polycrystalline gold electrode were reported using a variety of methodologies such as co-deposition and ECALE. Bulk electrolysis and cyclic voltammetry techniques were performed to obtain key parameters such as the deposition potential, the number of cycles, the deposition time and the effect of temperature. At the same time, chronoamperometry technique was used to determine the growth mechanism and the main structural characteristics of the deposited thin films. Single crystal surfaces needed complex systems to accumulate metals, so main point of this study was fundamentally targeted at more simple polycrystalline surfaces. At the same time, binary systems and thin films were created by the proposed dual approach.

## 2. Material and Method
### 2.1. Materials

Before starting the analysis, gold electrode was mechanically polished with 0.05 and 1.00 $\mu$m superfine alumina ($Al_2O_3$) powders and then cleaned electrochemically with successive cycling in 1.00 M sulfuric acid ($H_2SO_4$) solution from Sigma-Aldrich between $-0.20$ V and $+1.50$ V until a steady state current was obtained. 0.01 M ethylenediaminetetraacetic acid (EDTA) ($C_{10}H_{14}N_2Na_2O_8.2H_2O$) from Merck at pH 3.00 was used as a supporting electrolyte with copper (II) sulfate ($CuSO_4$), sodium sulfide ($Na_2S$) and zinc sulfate ($ZnSO_4$) from Sigma-Aldrich prepared in the concentration amount of 0.01 M. EDTA was used as a complexing agent to coordinate with Cu and Zn. All the other reagents were in analytical grade. At the beginning of

analysis, pure nitrogen ($N_2$) gas was passed from all of the prepared solutions for sufficient period of time to extract oxygen ($O_2$).

## 2.2. Instruments

Bulk electrolysis and cyclic voltammetry techniques were performed on CH Instruments CHI660C model potentiostat with a three electrode system consisting of foil coated Pt wire as a counter electrode to reduce polarization, silver/silver chloride (Ag/AgCl) as a reference electrode and Au electrode with 0.031 cm$^2$ area as a working electrode. Bulk electrolysis of Cu was done at +0.550 V for 7 minutes, S at −0.520 for 10 minutes, Zn at −0.750 V for Zn for 3 minutes. Cyclic voltammetry was applied between +1.500 V and −1.600 for both Cu and Zn. Chronoamperometry technique was performed between −0.050 V and −0.445 V for Cu +0.750 V and +0.100 V for Zn.

## 2.3. Mechanism of co-deposition and ECALE of CuS and ZnS

In the mechanism of co-deposition, EDTA which is suspended in the electrolyte works as the second phase particles and adsorbs the positively charged metal ions ($Cu^{2+}$ and $Zn^{2+}$). The metal ions surround the EDTA particles and the resulting complexes ($CuEDTA^{2-}$ and $ZnEDTA^{2-}$) arrive at the cathode taking action by the electrostatic attraction and the electrolyte convection. The remaining particles at the cathode surface discharge, and the three related interfacial energies including particle-electrolyte, particle-cathode and cathode-electrolyte keep the particles on the surface by the bonding force. The metal ions are deposited on the cathode surface around the particles mixing into the metallic deposits. In the case of S, anodic deposition is obtained on the anode surface.

Each element shows different UPD chemistry and it must be investigated to create its proper ECALE cycle. One stoichiometric layer of the proposed element is deposited in each cycle of a pure element, or a 1:1 compound. CuS or ZnS cycle is composed of several steps: initially a reductive UPD of Cu or Zn from a Cu or Zn cation solution, then oxidative UPD of S from a sulfide anion ($S^{2-}$) solution, and finally a second reductive UPD of Cu or Zn from a Cu or Zn cation solution. Separate solutions are used for each material and different potentials for each cycle step. The use of separate solutions and potentials gain advantage from extensive control over deposit growth, composition, and morphology. The cycle is repeated to form a thin film because the deposit thickness is a linear function of the number of cycles. Such a linear relation is a good indication of a layer by layer mechanism, and an atomic layer deposition process.

## 3. Results

### 3.1. UPD of Cu, S and Zn

Up to now, various electrochemical and surface characterization techniques have been used to estimate the mechanism of UPD. Among these techniques, cyclic voltammetry is extensively applied to distinguish the difference between the peak potentials of monolayer formation and bulk deposition. The first monolayer is formed from the described current peak at the potential $E > E_{rev}$ while the bulk deposition occurs at $E < E_{rev}$ where $E_{rev}$ defines the Nernstian equilibrium potential [17]. Nernstian potential of $Cu/Cu^{2+}$ is acquired at +0.28 V, $Zn/Zn^{2+}$ at −0.82 V. In Figure 1A, cyclic voltammogram of Au electrode in EDTA containing $CuSO_4$ (b) was compared with bare Au electrode behavior in EDTA (a), and bulk potential of Cu was obtained at −0.50 V (less than +0.28 V) while UPD potential was obtained at +0.55 V (more than +0.28 V) [18]. In Figure 1C, cyclic voltammogram of Au electrode in EDTA containing $ZnSO_4$ (b) was matched by bare Au electrode behavior in EDTA (a), and bulk potential of Zn was observed at −1.30 V (less than −0.82 V) during UPD potential was observed at −0.75 V (more than −0.82 V) [19]. In the case of S, cyclic voltammogram of Au electrode in EDTA containing $Na_2S$ (b) was evaluated along with bare Au electrode behavior in EDTA (a), but anodic potentials were estimated instead of cathodic potentials (Fig. 1B). The bulk potential of S was displayed at −1.00 V as UPD potential was displayed at −0.52 V, and similar UPD results to literature were reported [20].
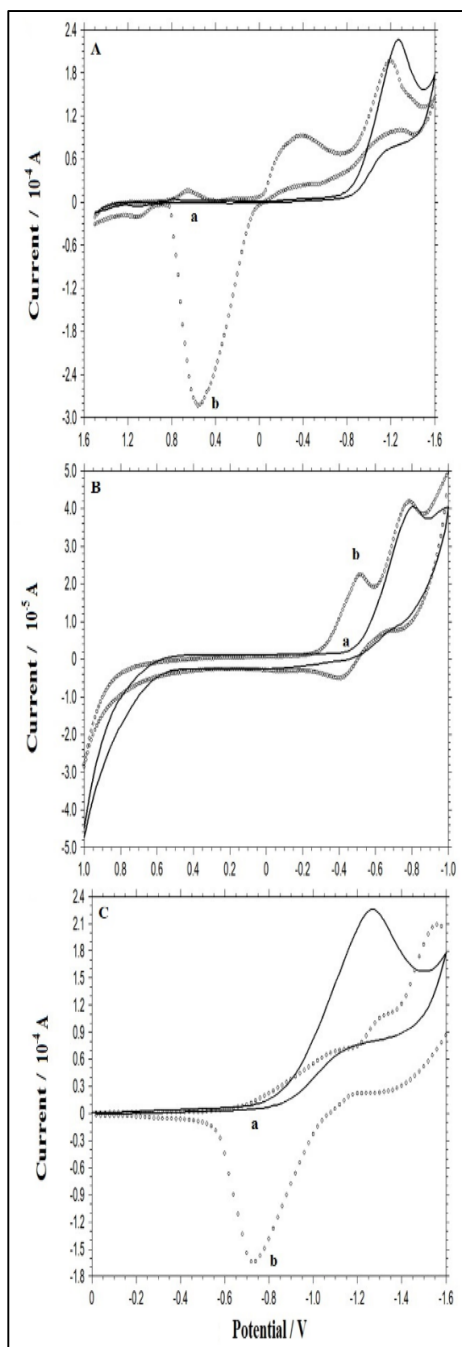
**Figure 1.** Cyclic voltammograms of **A)** bare Au (a) and Au in CuSO$_4$ (b) between +1.50 V and −1.60, **B)** bare Au (a) and Au in Na$_2$S (b) between +1.00 V and −1.00 V, **C)** bare Au (a) and Au in ZnSO$_4$ (b) between 0.00 V and −1.60 V at a scan rate of 100 mV s$^{-1}$.

## 3.2. Bulk electrolysis vs. cyclic voltammetry of CuS and ZnS

The basic UPD cycle can be repeated several times to obtain thicker deposits and such a choice can be made using various electrochemical techniques such as bulk electrolysis and cyclic voltammetry [21]. In the bulk electrolysis, an evaluation between the electrolysis time and the current density response of Au electrode in EDTA containing both CuSO$_4$ and ZnSO$_4$ were given in Table 1, and the maximum current density responses were gained on 7 min for Cu and 3 min for Zn (bold marked). Therefore, bulk electrolysis was performed at that time interval.

**Table 1**. The electrolysis time ($t$) vs. current density ($j$).

| $t$ (min) | $j_{Cu}$ (A m$^{-2}$) | $j_{Zn}$ (A m$^{-2}$) |
|---|---|---|
| 1 | −1.27 | −0.96 |
| 3 | −3.82 | **−7.64** |
| 5 | −5.73 | −2.87 |
| 7 | **−11.46** | −2.23 |
| 10 | −0.64 | −1.59 |

In the case of cyclic voltammetry, a comparison between the number of cycles of depositions and the current density ($j$) response of Au electrode in EDTA containing both CuSO$_4$ and ZnSO$_4$ were given in Table 2, and the maximum current density responses were taken in 7 cycles and 3 cycles for Cu and Zn (bold marked), respectively. Increasing current density resulted in increasing diffusion suggesting the denser, more compact flake structure [22]. Therefore, cyclic voltammetry technique was carried out in that cycle range.

**Table 2**. The number of cycles of depositions (#) vs. current density ($j$).

| # cycles | $j_{Cu}$ (A m$^{-2}$) | $j_{Zn}$ (A m$^{-2}$) |
|---|---|---|
| 1 | −33.44 | −1.27 |
| 3 | −41.40 | **−7.96** |
| 5 | −25.48 | −4.14 |
| 7 | **−47.77** | −2.87 |
| 10 | −31.85 | −3.18 |

Bulk electrolysis of Cu was applied at +0.55 V for 7 min while cyclic voltammetry was applied at a potential range of +0.80 V and −1.60 V for 7 cycles. On the other side, bulk electrolysis of Zn was performed at −0.75 V for 3 min while cyclic voltammetry was performed between +1.50 V and −1.60 V for 3 cycles. The methodological difference in the voltammetric behavior of Au electrode in EDTA containing $CuSO_4$ and $Na_2S$ (Figure 2A), and containing $Na_2S$ and $ZnSO_4$ (Figure 2B) was determined. No distinct peak difference was discovered for Cu in both techniques, but the UPD peak of Zn was lost in the event of bulk electrolysis. Therefore, the layer formation was accomplished by cyclic voltammetry.
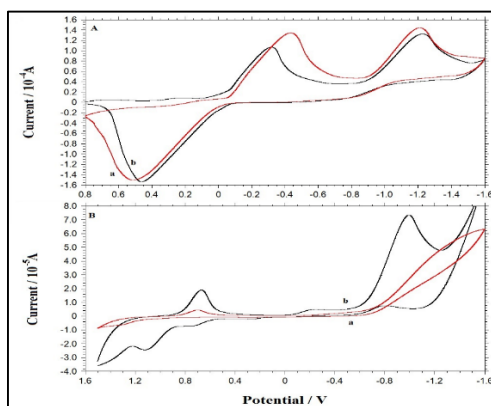


**Figure 2.** Cyclic voltammograms of **A)** bulk electrolyzed (a) and deposited Au (b) in $CuSO_4$ and $Na_2S$ between +0.80 V and −1.60 V, and **B)** bulk electrolyzed (a) and deposited Au (b) in $Na_2S$ and $ZnSO_4$ between +1.50 V and −1.60 V at a scan rate of 100 mV s$^{-1}$.

### 3.3. Co-deposition vs. ECALE of CuS and ZnS

Cyclic voltammetric responses of Au electrode using co-deposition method based on the deposition from the same solution of the target compound at a constant UPD potential, and using ECALE method based on the deposition of each element from their separate solutions at the UPD potential of each element were represented in Figure 3. In ECALE behavior of S over Cu modified Au electrode (b), the main UPD peaks of Cu (+0.55 V) and S (−0.52 V) disappeared, but in both co-deposition (a) and ECALE behavior of Cu over S modified Au electrode (c), both of the Cu and S UPD peaks were observed. A sharper result of Cu over S modified Au electrode than co-deposition technique presenting the layer formation of CuS by ECALE (Figure 3A). In the mechanism of CuS electrodeposition, Cu reduction ($Cu^{2+} + 2e^- = Cu_{UPD}$) and S oxidation ($S^{2-} = S_{UPD} + 2e^-$) occured as 1:1. An atomic layer of S was deposited on one layer of Cu, and one layer of Cu was deposited on one layer of S.

In the condition of Zn and S co-deposition (a), the most obvious UPD potential of Zn (−0.75 V) was obtained, but in both ECALE results S over Zn modified Au electrode (b) and Zn over S modified Au electrode (c), the broader UPD peaks of Zn were monitored. For the actual S UPD (−0.52 V), all surfaces shifted more positive potential (−0.25 V). According to these results, ZnS layer was created using co-deposition technique from the same solutions of Zn and S. In the mechanism of ZnS electrodeposition, Zn reduction ($Zn^{2+} + 2e^- = Zn_{UPD}$) and S oxidation ($S^{2-} = S_{UPD} + 2e^-$) occured as 1:1. An atomic layer of S was deposited on one layer of Zn, and one layer of Zn was deposited on one layer of S.
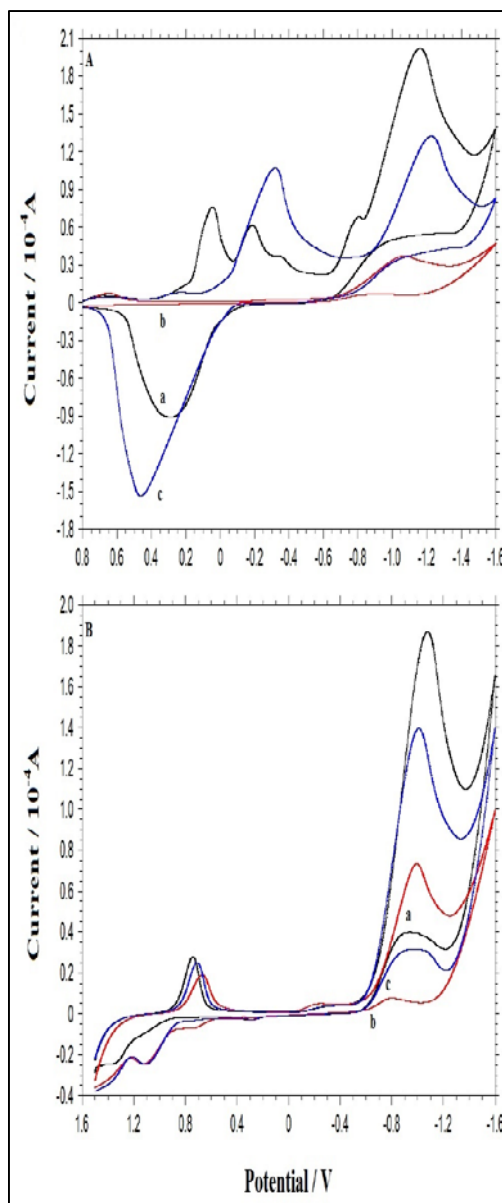
**Figure 3.** Cyclic voltammograms of **A)** Au using (a) Cu and S by co-deposition, (b) S over Cu by ECALE, (c) Cu over S by ECALE techniques between +0.80 V and −1.60 V, and **B)** Au using (a) Zn and S by co-deposition, (b) S over Zn by ECALE, (c) Zn over S by ECALE techniques between +1.50 V and −1.60 V at a scan rate of 100 mV s$^{-1}$.

### 3.4. The effect of bath temperature on UPD of CuS and ZnS

The nucleation and growth mechanism of electrodeposition can be influenced from different parameters such as the depositon potential, pH, concentration, scan rate, substrate and temperature. In the case of temperature, various effects are determined on active surface area and potential [23]. Therefore, the influence of bath temperature on thermodynamics and kinetics of nucleation and growth onto Au was studied, and the bath temperature was changed from 25 ºC to 40 ºC to examine the change of composition and microstructure of the deposits. In Figure 4, the current intensities of bare Au electrode in EDTA containing CdSO$_4$ (A), Cu and S co-deposited Au electrode (B), S over Cu modified Au electrode (C), and Cu over S modified Au electrode (D) in EDTA containing CuSO$_4$ and Na$_2$S were compared. When the bath temperature increased from 25 ºC to 40 ºC (d→a), the intensity of the peaks increased randomly for all surfaces. The maximum current response decreased at Cu and S co-deposited Au electrode (5.00 × 10$^{-5}$ A) and reached its highest point (3.50 × 10$^{-4}$ A) at Cu over S modified Au electrode. A gradual rise from 25 ºC to 35 ºC was observed at Cu over S modified Au electrode, but a continuos tendency of increase and decrease was obtained from A to C. Therefore, the layer formation of CuS was carried out using ECALE technique as in UPD results of Cu over S modified Au electrode, and the increase of the bath temperature improved the crystallinity of the CuS deposit [24].
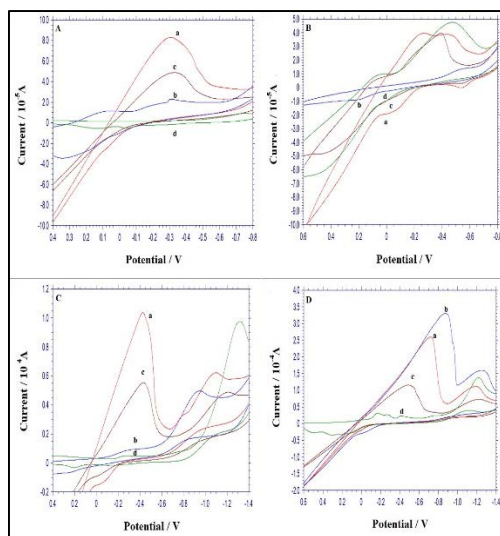
**Figure 4.** Cyclic voltammograms of **A)** bare Au, **B)** Au using Cu and S by co-deposition, **C)** Au using S over Cu by ECALE, and **D)** Au using Cu over S by ECALE techniques between +0.60 V and −1.40 V at a scan rate of 100 mV s$^{-1}$ and at a bath temperature of (a) 40 ºC, (b) 35 ºC, (c) 30 ºC, (d) 25 ºC.

Figure 5 demonstrated the current intensity changes of bare Au electrode in EDTA containing $ZnSO_4$ (A), Zn and S co-deposited Au electrode (B), Zn over S modified Au electrode (C), and S over Zn modified Au electrode (D) in EDTA containing $ZnSO_4$ and $Na_2S$. As the bath temperature increased from 25 ºC to 40 ºC (d→a), the intensity of the peaks increased randomly for all surfaces. The maximum peak currents (between $2.00 \times 10^{-5}$ A and $3.00 \times 10^{-5}$ A) were almost same even though the surfaces were formed by different techniques. A progressive jump was monitored at only Zn and S co-deposited Au electrode, but all other surfaces showed an irregular upward trend. Therefore, the layer formation of ZnS was carried out using co-deposition technique as in UPD results of Zn and S co-deposited Au electrode, and the bath temperature had an influence on the composition of the deposited films.
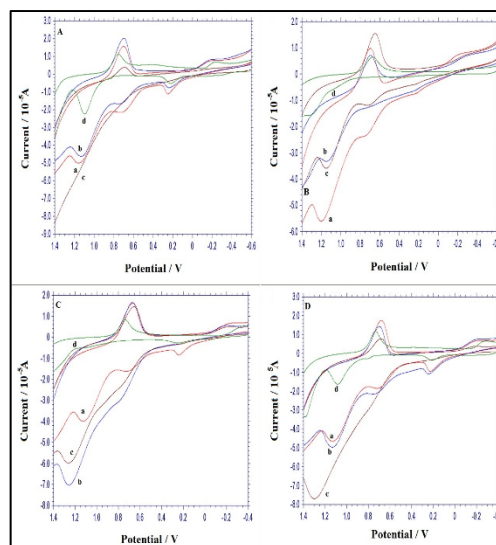


**Figure 5.** Cyclic voltammograms of **A)** bare Au, **B)** Au using Zn and S by co-deposition, **C)** Au using Zn over S by ECALE, and **D)** Au using S over Zn by ECALE techniques between +1.40 V and −0.40 V at a scan rate of 100 mV s$^{-1}$ and at a bath temperature of (a) 40 ºC, (b) 35 ºC, (c) 30 ºC, (d) 25 ºC.

### 3.5. Kinetics of the electrodepositions of CuS and ZnS

Copper monolayer formation onto Au polycrystalline electrode is independent from the crystalline nature of the Au electrode. When a copper monolayer is grown up during the UPD, a difference in the corresponding current transients occur. Potentiostatic current density transients during nucleation and growth onto Au vary at different potentials. Therefore, different mechanisms should be involved in each case of the monolayer formation. In a more detailed analysis of the transients, the polycrystalline Au electrode represents more similarities than actual differences with respect to the single crystal electrode. Current-time transients from chronoamperometry experiments are compared with the theoretical models to characterize the type of nucleation for deposits [25]. In order to describe totally the shape of the transients, the model ($j_{total} = j_{AD} + j_{2D}$) explored by Hölzle et al. is used where the overall current density for the electrodeposition process ($j_{total}$) is the linear sum of a Langmuir-type adsorption term ($j_{AD}$) and a 2D nucleation process ($j_{2D}$) [26].

In Figure 6, chronoamperometric results of bare Au (a) and coated Au (b) in EDTA containing CuSO$_4$, coated Au using Cu and S by co-deposition (c), and coated Au using Cu over S by ECALE (d) techniques in EDTA containing CuSO$_4$ and Na$_2$S were estimated. In all conditions, the current density decreased as a function of elapsing time ($t < 0.03$ s), right from the start of the transient resulted in no nucleation model giving a clear description of the transient shape. For $t > 0.03$ s, the shape of transient supported the formation and growth of 2D nuclei, limited by ad-atom incorporation. As it could be seen in Figure 6 (a→b), a current decrease appeared in Cu monolayer formation, and a current increase was observed by Cu and S co-deposited Au electrode (b→c) similar to literature [26]. As a result, chronoamperometry process of CuS layer proceeded by a two-step mechanism involving Langmuir-type adsorption accompanied by nucleation and two dimensional growth, and Cu deposition was determined by the Hölzle model ($j_{total} = j_{AD} + j_{2D}$) in which the electrodeposition process ($j_{total}$) was the linear sum of a Langmuir-type adsorption term ($j_{AD}$) and a 2D nucleation process ($j_{2D}$).
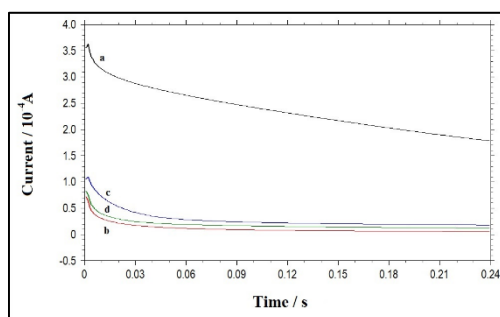


**Figure 6.** Chronoamperometric behaviors of **a)** bare Au in EDTA, **b)** Au in CuSO$_4$, **c)** Au using Cu and S by co-deposition, **d)** Au using Cu over S by ECALE techniques in CuSO$_4$ and Na$_2$S between −0.050 V and −0.445 V.

In order to analyze the experimental data by usual procedures, the plots of $j$ vs. $t^{-1/2}$ (A) and $j$ vs. $t^{1/2}$ (B) for bare Au (a) and coated Au (b) in EDTA containing CuSO$_4$, coated Au for using Cu and S by co-deposition (c), and coated Au for using Cu over S by ECALE (d) techniques in EDTA containing CuSO$_4$ and Na$_2$S recorded between −0.050 V and −0.445 V were given in Figure 7.
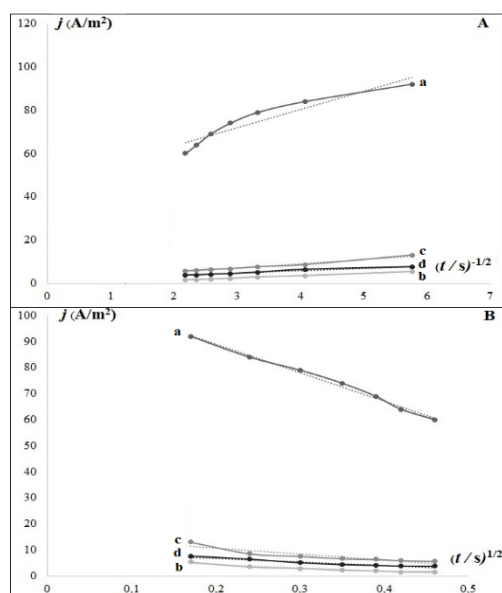


**Figure 7.** The plots of **A)** $j$ vs. $t^{-1/2}$ and **B)** $j$ vs. $t^{1/2}$ indicating the current transients of bare Au (a), Au in CuSO$_4$ (b), Au using Cu and S by co-deposition (c), Au using Cu over S by ECALE (d) techniques in CuSO$_4$ and Na$_2$S recorded between −0.050 V and −0.445 V, see in Figure 6.

As it was seen from Table 3, the current density response of bare Au electrode was directly proportional to $t^{1/2}$ due to the metal ion behavior of Au while all other monolayered surfaces were directly proportional to $t^{-1/2}$. Therefore, resulting straight line from Figure 7A (b→d) showed a diffusion-controlled process according to the Cottrell equation [27] and the higher the slope of graph was obtained in Figure 7A (c) because of the current increase by Cu and S co-deposited Au electrode. Diffusion coefficients ($D$) were also calculated as 1.00, 3.37, 1.10 ($\times 10^{-8}$ cm$^2$/s) from b to d, respectively, and the highest diffusivity was obtained at Cu and S co-deposited Au electrode.

**Table 3**. Equations and R-squared values for the plots of of $j$ vs. $t^{-1/2}$ and $j$ vs. $t^{1/2}$.

| deposition | $j$ vs. $t^{-1/2}$ | $j$ vs. $t^{1/2}$ |
|---|---|---|
| a | y = 8.50x + 46.41<br>$R^2$ = 0.90 | y = -109.5x +111.0<br>$R^2$ = 0.99 |
| b | y = 1.99x + 1.12<br>$R^2$ = 0.98 | y = -22.6x + 15.2<br>$R^2$ = 0.85 |
| c | y = 1.14x + 1.25<br>$R^2$ = 0.97 | y = -13.9x + 9.62<br>$R^2$ = 0.94 |
| d | y = 1.08x – 0.86<br>$R^2$ = 0.99 | y = -12.8x + 6.97<br>$R^2$ = 0.92 |

Figure 8 demonstrated chronoamperometric responses of coated Au (a) in EDTA containing $ZnSO_4$, coated Au using Zn and S by co-deposition (b), and coated Au using Zn over S by ECALE (c) techniques in EDTA containing $ZnSO_4$ and $Na_2S$. A current decline (a→b) was observed by Zn and S co-deposited Au electrode, but when Zn monolayer was formed over S modified Au electrode (c), the current increased again. The general curves in the UPD range had a monotonous character approaching close to zero quickly. At later times, the current seemed to be independent on the deposition time. Such an observation was made by the Despic and Pavlovic model referred to a repetitive 2D layer growth in which smooth deposit reproduced the original surface morphology [28]. Therefore, it proceeded by a 2D nucleation and growth mechanism.

In Figure 8, inset, the plots of $j$ vs. $t^{-1/2}$ for coated Au (a) in EDTA containing $ZnSO_4$, coated Au using Zn and S by co-deposition (b), and coated Au using Zn over S by ECALE (c) techniques in EDTA containing $ZnSO_4$ and $Na_2S$ recorded between +0.75 V and +0.10 V were indicated. The resulting linearity on all surfaces showed a diffusion-controlled process according to the Cottrell equation. Diffusion coefficients were calculated as 8.43, 0.28, 1.65 ($\times 10^{-8}$ cm$^2$/s) from a to c, respectively, and the higher diffusivity than Zn and S co-deposited Au electrode was obtained at Zn over S deposited Au electrode by ECALE technique. For the electrodeposition of ZnS (b and c), the diffusion coefficients ($D \sim 1/\eta$) based on the slopes declined normally because of the absolute viscosity ($\eta$) which was greater for deposits in comparison with free metals (a).
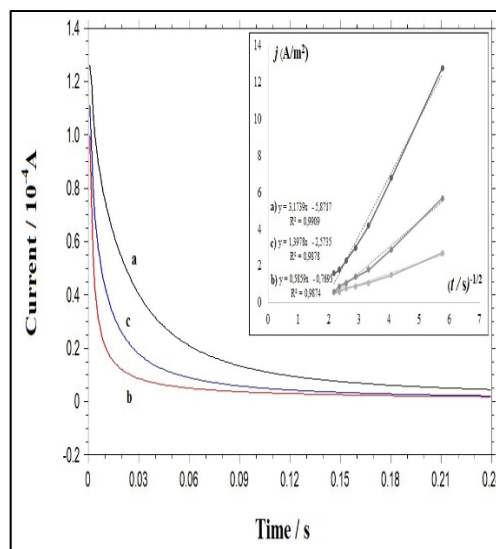


**Figure 8.** Chronoamperometric behaviors of **a)** Au in $ZnSO_4$, **b)** Au using Zn and S by co-deposition, **c)** Au using Zn over S by ECALE techniques in $ZnSO_4$ and $Na_2S$ between +0.75 V and +0.10 V. Inset: the plots of $j$ vs. $t^{-1/2}$ indicating the current transients.

## 4. Discussion and Conclusion

An easy, one-step procedure for the electrodeposition of CuS and ZnS was developed. Development of the binary system composed of co-deposition and ECALE techniques gained advantage from comparable point of view. Chosen two methods to produce semiconducting CuS and ZnS thin films were described in depth onto polycrystalline electrodes. A variety of electrochemical deposition processes such as bulk electrolysis and cyclic voltammetry were used to select the ideal deposition method. The influence of bath temperature on UPD was studied to estimate the quality and crystallinity of deposits, and almost same results with the UPD responses of CuS and ZnS were obtained in various bath temperatures. The decision on the kinetic behaviors of deposits was made by chronoamperometry technique, and two-step mechanism involving adsorption accompanied by nucleation and growth was obtained. To conclude, UPD was applied on pure metals and their deposits through the study, so that the recommended method may arouse as a model in both semiconducting industry and environmental science.

**References**

[1] Oviedo, O.A., Reinaudi, L., Garcia, S.G., Leiva, E.P.M. 2016. Underpotential deposition: from fundamentals and theory to applications at the nanoscale. Scholz F., ed. Springer International Publishing, Switzerland. DOI: 10.1007/s10008-016-3222-7.

[2] Mascaro, L.H., Santos, M.C., Machado, S.A.S., Avaca, L.A. 2002. Voltammetric and Rotating Ring-Disk Studies of the Influence of Anions in the Underpotential Deposition of Zinc on Platinum. Journal of the Brazilian Chemical Society, Vol. 13, p. 529-534. DOI: 10.1590/S0103-50532002000400019.

[3] Gregory, B.W., Stickney, J.L. 1991. Electrochemical atomic layer epitaxy (ECALE). Journal of Electroanalytical Chemistry, Vol. 300, p. 543-561. DOI: 10.1016/0022-0728(91)85415-L.

[4] Liang, X., Jayaraju, N., Thambidurai, C., Zhang, Q., Stickney, J.L. 2011. Controlled elec-trochemical formation of GexSbyTez using atomic layer deposition (ALD). Chemistry of Materials, Vol. 23, p. 1742-1752. DOI: 10.1021/cm102672j.

[5] Öznülüer, T., Erdoğan, İ.Y., Şişman, İ., Demir, Ü. 2005. Electrochemical atom-by-atom growth of PbS by modified ECALE method. Chemistry of Materials, Vol. 17, p. 935-937. DOI: 10.1021/cm048246g.

[6] Zhu, W., Liu, X., Liu, H., Tong, D., Yang, J., Peng, J. 2010. Coaxial heterogeneous structure of $TiO_2$ nanotube arrays with CdS as a superthin coating synthesized via modified electrochemical atomic layer deposition. Journal of the American Chemical Society, Vol. 132, p. 12619-12626. DOI: 10.1021/ja1025112.

[7] Noyhouzer, T., Mandler, D. 2011. Determination of low levels of cadmium ions by the under potential deposition on a self-assembled monolayer on gold electrode. Analytica Chimica Acta, Vol. 684, p. 1-7. DOI: 10.1016/j.aca.2010.10.021.

[8] Aramataa, A., Taguchi, S., Fukudaa, T., Nakamuraa, M., Horanyi, G. 1998. Underpotential deposition of zinc ions at single crystal electrodes and the effect of the adsorbed anions. Electrochimica Acta, Vol. 44, p. 999-1007. DOI: 10.1016/S0013-4686(98)00204-7.

[9] Giaccherini, A., Cinotti, S., Guerri, A., Carla, F., Montegrossi, G., Vizza, F., Lavacchi, A., Felici, R., Di Benedetto, F., Innocenti, M. 2017. Operando SXRD study of the structure and growth process of Cu 2 S ultra-thin films. Scientific Reports, Vol. 7, p. 1615. DOI: 10.1038/s41598-017-01717-0.

[10] Bozzini, B., Baker, M.A., Cavallotti, P.L., Cerri, E., Lenardi, C. 2000. Electrodeposition of ZnTe for Photovoltaic Cells. Thin Solid Films, Vol. 361, p. 388-395. DOI: 10.1016/S0040-6090(99)00808-1.

[11] Pauporte, T., Lincot, D. 2000. Electrodeposition of semiconductors for optoelectronic devices: results on zinc oxide. Electrochimica Acta, Vol. 45, p. 3345-3353. DOI: 10.1016/S0013-4686(00)00405-9.

[12] Heo, P., Ichino, R., Okido, M. 2006. ZnTe electrodeposition from organic solvents. Electrochimica Acta, Vol. 51, p. 6325-6330. DOI: 10.1016/j.electacta.2006.04.016.

[13] Dogel, J., Freyland, W. 2003. Layer-by-layer growth of zinc during electrodeposition on Au(111) from a room temperature molten salt. Physical Chemistry Chemical Physics, Vol. 5, p. 2484-2487. DOI: 10.1039/B303388K.

[14] Alanyalıoğlu, M., Çakal, H., Öztürk, A.E., Demir, Ü. 2001. Electrochemical studies of the effects of pH and the surface structure of gold substrates on the underpotential deposition of sulfur. The Journal of Physical Chemistry B, Vol. 105, p. 10588-10593. DOI: 10.1021/jp004227s.

[15] Mahalingam, T., John, V.S., Rajendran, S., Ravi, G., Sebastian, P.J. 2002. Annealing studies of electrodeposited zinc telluride thin films. Surface and Coatings Technology, Vol. 155, p. 245-249. DOI: 10.1016/S0257-8972(02)00117-2.

[16] Short, A., Jewell, L., Bielecki, A., Keiber, T., Bridges, F., Carter, S., Alers, G. 2014. Structure in multilayer films of zinc sulfide and copper sulfide via atomic layer deposition. Journal of Vacuum Science & Technology A, Vol. 32, p. 01A125. DOI: 10.1116/1.4847956.

[17] Sudha, V., Sangaranarayanan, M.V. 2005. Underpotential deposition of metals – Progress and prospects in modelling. Journal of Chemical Sciences, Vol. 117, p. 207-218. DOI: 10.1007/BF02709289.

[18] Chiu, Y.D., Dow, W.P., Liu, Y.F., Lee, Y.L., Yau, S.L., Huang, S.M. 2011. Copper Underpotential Deposition on Gold in the Presence of Polyethylene Glycol and Chloride. International Journal of Electrochemical Sciences, Vol. 6, p. 3416-3426.

[19] Taguchi, S., Kondo, M., Mori, H., Aramata, A. 2013. Formation of zinc–oxianion complex adlayer by underpotential deposition of Zn on Au(1 1 1) electrode: Preferential formation of zinc monohydrogen phosphate complex in weakly acidic solutions. Electrochimica Acta, Vol. 111, p. 642-655. DOI: 10.1016/j.electacta.2013.07.217.

[20] Biçer, M., Aydın, A.O., Şişman, İ. 2010. Electrochemical synthesis of CdS nanowires by underpotential deposition in anodic alumina membrane templates. Electrochimica Acta, Vol. 55, p. 3749-3755. DOI: 10.1016/j.electacta.2010.02.015.

[21] Innocenti, M., Cinotti, S., Bencista, I., Carretti, E., Becucci, L., Di Benedetto, F., Lavacchi, A., Foresti, M.L. 2014. Electrochemical Growth of Cu-Zn Sulfides of Various Stoichiometries. Journal of The Electrochemical Society, Vol. 161, p. D14-D17. DOI: 10.1149/2.021401jes.

[22] Rusi, M.S.R. 2016. Effects of Electrodeposition Mode and Deposition Cycle on the Electrochemical Performance of $MnO_2$-NiO Composite Electrodes for High-Energy-Density Supercapacitors. Plos One, Vol. 11, p. e0154566. DOI: 10.1371/journal.pone.0154566.

[23] Palomar Pardave, M., Aldane Gonzalez, J., Botello, L.E., Arce Estrada, E.M., Ramirez Silva, M.T., Mostany, J., Romero Romo, M. 2017. Influence of Temperature on the Thermodynamics and Kinetics of Cobalt Electrochemical Nucleation and Growth. Electrochimica Acta, Vol. 241, p. 162-169. DOI: 10.1016/j.electacta.2017.04.126.

[24] Cheng, S., Chen, G., Chen, Y., Huang, C. 2006. Effect of deposition potential and bath temperature on the

electrodeposition of SnS film. Optical Materials, Vol. 29, p. 439-444. DOI: 10.1016/j.optmat.2005.10.018.

[25] Tylka, M.M., Willit, J.L., Williamson, M.A. 2017. Electrochemical Nucleation and Growth of Uranium and Plutonium from Molten Salts. Journal of The Electrochemical Society, Vol. 164, p. H5327-H5335. DOI: 10.1149/2.0471708jes.

[26] Garfias-Garcia, E., Palamor-Pardave, M., Romero-Romo, M., Ramirez-Silva, M.T., Batina, N. 2007. Kinetic Mechanism of Copper UPD Nucleation and Growth on Mono and Polycrystalline Gold. ECS Transactions, Vol. 3, p. 35-43. DOI: 10.1149/1.2795610.

[27] Cottrell, F.G. 1902. Der reststrom bei galvanischer polarisation, betrachtet als ein diffusionsproblem. Zeitschrift für Physikalische Chemie, Vol. 42, p. 385-431. DOI: 10.1515/zpch-1903-4229.

[28] Dogel, J. 2004. Electrochemical SPM Study of 2D and 3D Phase Formation of Zn at the Ionic Liquid /Au(111) Interface. Universitätsverlag Karlsruhe, Karlsruhe.